Study of the solidification behaviour of metallurgical slags using the Single Hot Thermocouple Technique

Jeferson L. Klug [1,2], R. Hagemann [2], Nestor C. Heck [1], Antônio C. F. Vilela [1], Hans P. Heller [2], Piotr R. Scheller [2]*

1) Federal University of Rio Grande do Sul, Brazil

2) Freiberg University of Mining and Technology, Germany

Abstract: With the Single Hot Thermocouple Technique (SHTT) the solidification behaviour of metallurgical slags has been studied using the apparatus of the Freiberg University of Mining and Technology, Germany, in cooperation with the Federal University of Rio Grande do Sul, Brazil. With this technique, which is suitable to build TTT or CCT diagrams, the sample is put on a thermocouple tip and can be heated or cooled at very high rates (> 3000 °C/min) due to the low mass of the system. One advantage is to allow *in situ* observation of melting and solidification under various thermal conditions.

The motivation for this work is to provide basic information related to crystallisation control, for the development of fluorine-free mould slags for continuous casting of steel.

Slags in the systems CaO-Al_2O_3, CaO-SiO_2, CaO-SiO_2-TiO_2, and CaO-SiO_2-TiO_2-Na_2O were studied, analysing the kinetics of crystals growth and crystals morphology.

Following findings are reported: (i) for the slag CS (%CaO/%SiO_2 = 0.7) no crystal is observed during continuous cooling even to low cooling rates, but on the other hand intense crystallisation is obtained when increasing the temperature after reaching a particular range of lower temperatures; (ii) it was observed that the longer the duration of the superheating, the longer the incubation times for one slag CST (41%CaO, 29%SiO_2, 30%TiO_2) which has high *liquidus* temperature; (iii) the addition of Na_2O into the CaO-SiO_2-TiO_2 slag system shortens intensely the crystals incubation times at TTT diagrams to the range of seconds. Therefore Na_2O acts as crystallisation accelerator.

Keywords: Single Hot Thermocouple Technique, Metallurgical slags, Fluorine-free mould fluxes, Slab casting

1. Introduction

To control the phenomena in the mould during continuous casting is essential to the success of the process. The mould slag i.e. the mould flux which was melted in the mould is one of the most important slags in the melting shop. The choice of the mould flux is a difficult task because of the complicated nature of the powder composition, and because the mould powder has many important functions. Due to the complex requirements in the industrial process the choice is based on trials in the caster followed by investigations on the quality of the slabs [1-3].

Commercial mould powders contain fluorine, usually as calcium fluoride (CaF_2). However, there is a clear trend in industry to eliminate fluorine from slags which are used during production of steel. The main problem related to the development of fluorine-free mould powders for slab casting is how to control the heat transfer between steel shell and mould. The crystallisation of cuspidine ($3CaO.2SiO_2.CaF_2$) from F-bearing mould flux is thought to be the most

effective way for heat transfer control. Although the mechanism of the heat transfer control by the crystallisation of cuspidine has not been determined yet, two ideas have been proposed. One is that radiation heat flux is decreased by scattering at the boundary between the crystalline and the liquid layers and the other is that total heat flux is decreased by the large thermal resistance of the air gap formed as a result of the solidification shrinkage. Anyway, cuspidine crystallisation from mould slag has the great effect on heat transfer control [4].

Several papers have been reporting possibilities to replace the phase cuspidine regarding the heat transfer control function, by the formation of different crystals. Some papers indicate that TiO_2-bearing raw materials can be used by formation of TiO_2 crystals [4-6]. And besides, there are also other works with reports on the solidification behaviour of mould fluxes without fluorine or with lower fluorine content, considering different crystals, like $Na_2O.CaO.3SiO_2$ [7]; $Na_2O.2CaO.3SiO_2$ [8]; $CaSiO_3$,$Ca_3Si_2O_7$ and Ca_2SiO_4 [9]; CaB_2SiO_7 and $CaAl_{14}B_2[SiO_4]_8$ [10].

The Single Hot Thermocouple Technique (SHTT) can be used to build TTT diagrams. With this technique the sample is put on one thermocouple tip, heated and cooled at the desired rates. One feature of the technique is to allow *in situ* observation of melting and solidification under various thermal conditions. Due to the low mass of the system (sample and thermocouple) high heating and cooling rates (> 3000 °C/min) can be easily obtained. Besides SHTT, using the hot thermocouple technique another experimental mode is also possible: the Double Hot Thermocouple Technique (DHTT). With the DHTT the solidification behaviour can be observed in situ applying temperature gradients, simulating the conditions during continuous casting. In this mode the slag sample is placed between the tips of two thermocouples. Both sides can be controlled independently and mould-like temperature gradients or heat peaks can be applied [11].

The objective of the present work is to use the Single Hot Thermocouple Technique to perform a basic study evaluating the crystallisation behaviour of slags in the systems $CaO\text{-}Al_2O_3$, $CaO\text{-}SiO_2$, $CaO\text{-}SiO_2\text{-}TiO_2$, and $CaO\text{-}SiO_2\text{-}TiO_2\text{-}Na_2O$. The motivation for this study is to provide information related to crystallisation control, for the development of fluorine-free mould slags for continuous casting of steel.

2. Experimental

2.1 Materials and samples preparation

The slags were produced from reagent grade $CaCO_3$, SiO_2 , TiO_2 , Na_2CO_3 and Al_2O_3 . These substances were pre-melted in graphite crucibles with an induction furnace and subsequently milled, decarburized, and analysed through X-ray fluorescence (XRF). Carbon was analysed with LECO CS 244. The results are at Table 1.

Table 1. Composition of the slags used for the SHTT [%wt.]. B is the ratio $\%CaO/\%SiO_2$.

	%CaO	$\%SiO_2$	$\%TiO_2$	$\%Na_2O$	$\%Al_2O_3$	%C	B
CA	43.7				56.3	0.074	
CS	41.7	58.3				0.063	0.7
CST_1	41.1	29.1	29.8			-	1.4
CST_2	35.6	46.3	18.1			0.590	0.8
CSTNA_1	33.6	41.3	16.5	7.1	1.5	0.073	0.8
CSTNA_2	30.1	46.8	16.4	5.4	1.3	0.034	0.6
CSTNA_3	31.6	48.1	15.5	3.7	1.1	0.032	0.7
CSTNA_4	30.9	42.3	15.2	6.4	5.2	0.038	0.7

2.2. The Hot Thermocouple Technique

The apparatus used in the present work was constructed in the Institute of Iron and Steel Technology of the Freiberg University of Mining and Technology, Germany [11]. A schematic view is given at Figure 1. It consists basically of two systems: an observation system and a thermocouple system. In a vacuum chamber there are two water-cooled inserts left and right. Both of them hold a B-type thermocouple at tips. Each thermocouple is connected to a separate thermocouple controller. The material under study is melted directly on thermocouple inside the vaccum chamber. The thermocouples remains inside an additional heating, i.e. a kanthal coil which reduces heat losses from the sample to the surroundings.

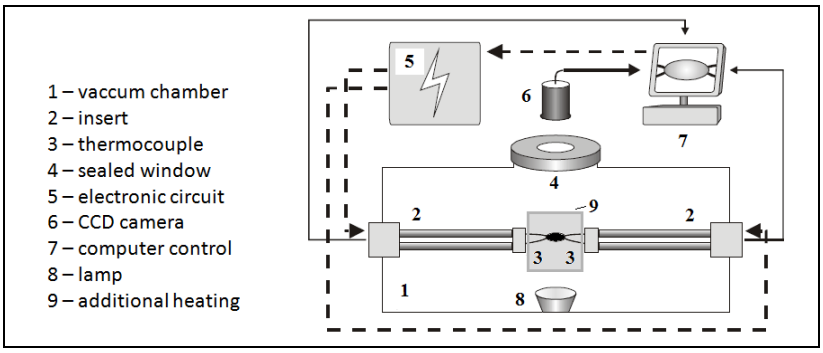

Figure 1. Schematic view of the experimental set-up.

With this experimental set-up it is possible to measure the sample temperature with a thermocouple while it is heated simultaneously. A computer manages the two thermocouple controllers, controlling individually heating and cooling conditions. A software superimposes information about time, temperature and sample image into videos files in a real-time system.

Thermocouples are built using two platinum wires of 0.5 mm diameter, and length of ca. 25 mm: Pt30Rh (Plus) and Pt6Rh (minus). The tips of the wires are welded with a special technique. The weld should be carefully done in order to minimize measurement errors; a typical thermocouple can be seen at Figure 2(b).

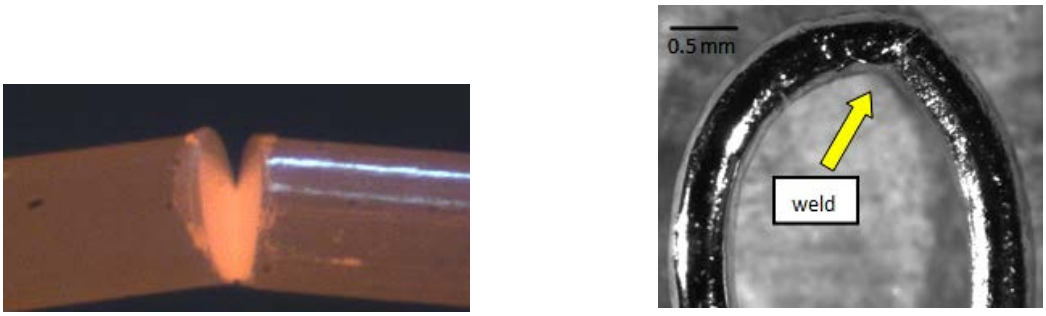

(a) (b)

Figure 2. (a) beginning of the welding (Pt30Rh wire and Pt6Rh wire), (b) tip of one typical thermocouple showing the region where slags samples are melted.

The accuracy of the apparatus was checked measuring the crystallisation temperature of CaF_2, Na_2SO_4 and K_2SO_4. The crystallisation temperature – $T_{cryst.}$ – is defined here as the temperature where the first crystals can be observed for a

particular cooling rate. With the substances in the vacuum chamber it was applied 5 min of vacuum at 10 mbar. Then, the vessel was filled with Ar, maintaining a flux of 300 l/h during the measurements. Afterwards, the substances were melted 100°C above their melting points and cooled at 30 °C/min. Their melting points are [12]:
CaF_2 - 1418 °C, Na_2SO_4 - 884 °C , K_2SO_4 - 1069 °C .

The differences between the literature melting points [12] and the $T_{cryst.}$ are indicated at Figure 3. Twelve experiments were performed for each substance (experiments 1-6 with the left thermocouple and experiments 7-12 with the right thermocouple, see Figure 1).

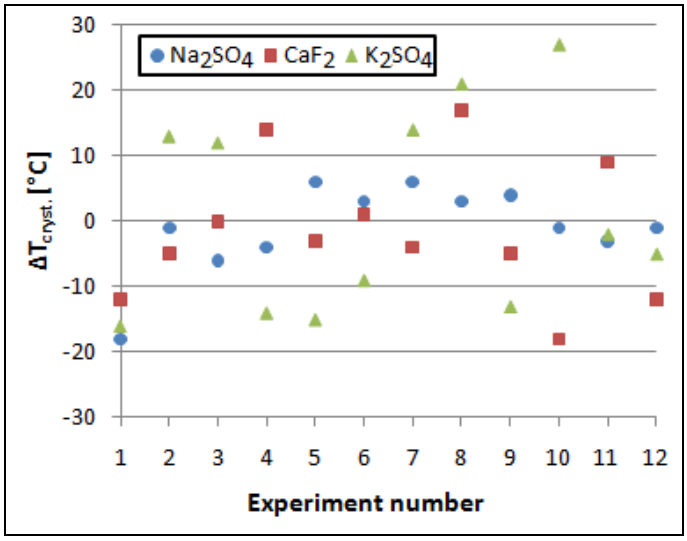

Figure 3. Comparison between literature [12] and results from the present work. $\Delta T_{cryst.}$ is the difference between the literature melting point and the crystallisation temperature which was measured by SHTT.

Assuming a normal distribution for $\Delta T_{cryst.}$ average values and standard deviations can be calculated, see Table 2. The average values are very close to the melting points from literature and the scattering is low. The small observed differences can be related to particular conditions for heterogeneous nucleation. For CaF_2 and Na_2SO_4 the crystallisation is intense and takes place suddenly; in this situation it is easy to define accurately the beginning of the crystallisation. For K_2SO_4 , the substance which presents the higher standard deviation, the crystallisation is not so intense and normally takes several seconds to finish.

Table 2. Comparison between literature [12] melting points and crystallisation temperatures (measured by SHTT, for each substance twelve measurements were performed).

Substance	m.p. literature [12]	average $T_{cryst.}$	standard deviation $T_{cryst.}$
CaF_2	1418 °C	1417 °C	10.6 °C
Na_2SO_4	884 °C	883 °C	6.6 °C
K_2SO_4	1069 °C	1071 °C	15.4 °C

The results summarized at Table 2 were obtained through video file analysis. The apparatus also registers the evolution of temperature with time, in a similar manner to differential thermal analysis (DTA). It was verified during calibration that the visually observed crystallisation corresponds to peaks at the T *versus* t diagrams. Examples at Figures 4 and 5, where the energy liberation rate during cooling is sufficiently high to produce observable peaks. The

"first crystals" at the diagrams means the temperature where it is possible to see the first ones.

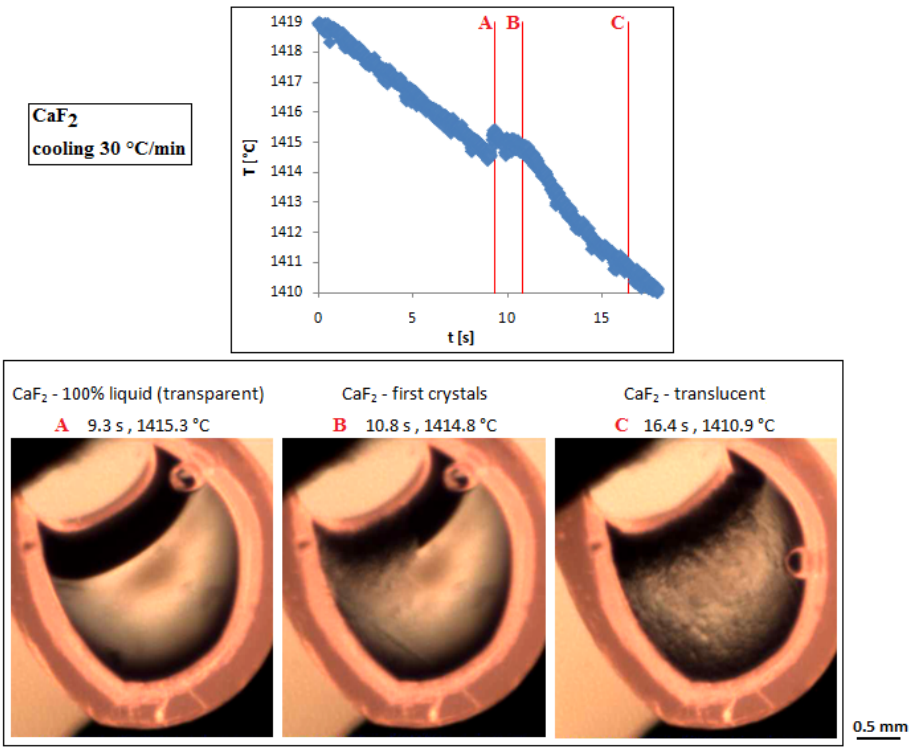

Figure 4. Relation between CaF_2 crystallisation peak at T *versus* t diagram (above) and the observed start of crystallisation (below).

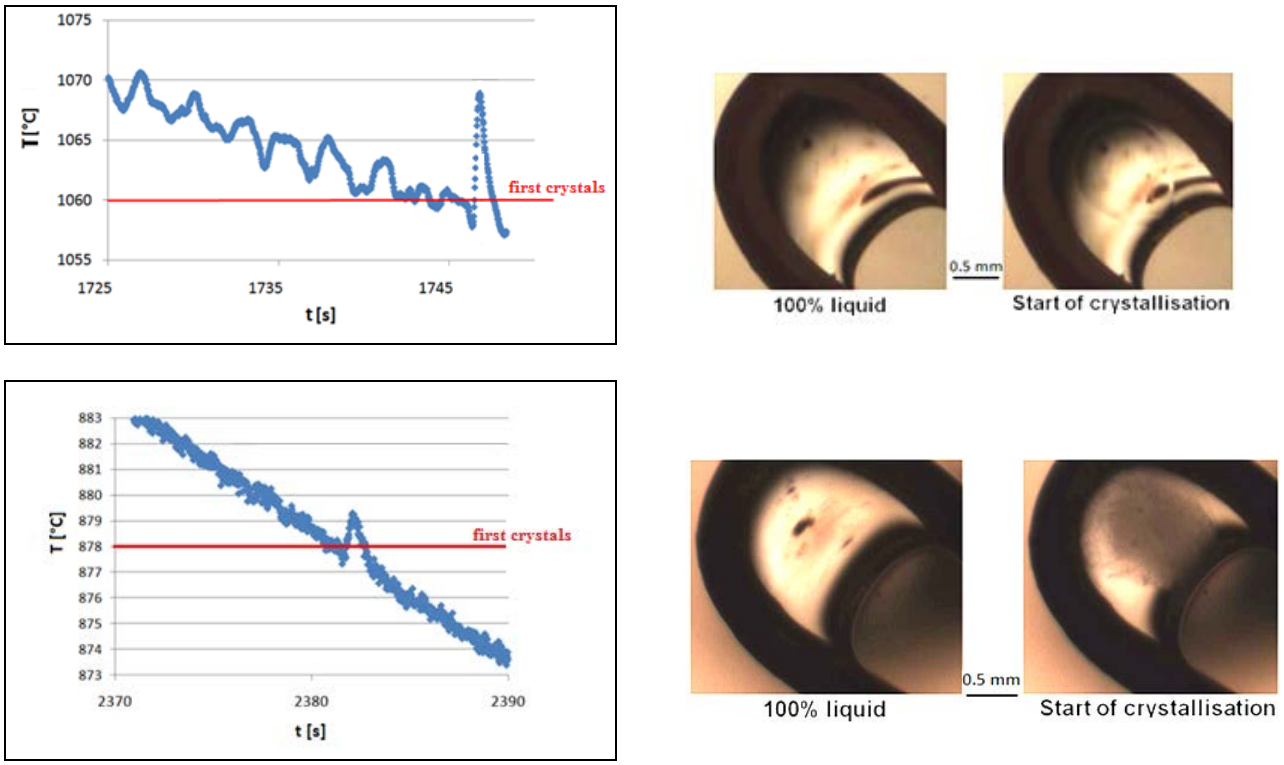

Figure 5. T *versus* t diagrams for K_2SO_4 (above) and Na_2SO_4 (below), with the typical crystallisation at right. Cooling at 30 °C/min.

2.3 Experimental procedure

To execute the experiments slags small portions of premelted slags (typically 5-10 mg) are pressed and put on the thermocouple tip. With the substances in the vacuum chamber it is applied 5 min of vacuum at 10 mbar. Then, the vessel is filled with Ar, maintaining a flux of 300 l/h during the measurements. The additional heating is turned on, maintaining ca. 500 °C around the thermocouple. The slag samples are heated and melted directly on the thermocouple tip, using one thermocouple per slag sample. During the operation lime slurry is maintained at the gas exit. The experiments are registered with video files.

For time-temperature-transformation (TTT) diagrams, after melting very high cooling rates (higher than 3000 °C/min) are applied like illustrated at Figure 6(a). From this point the incubation time is measured by direct observation. For continuous-cooling-transformation (CCT) diagrams the thermal cycle is like illustrated at Figure 6(b).

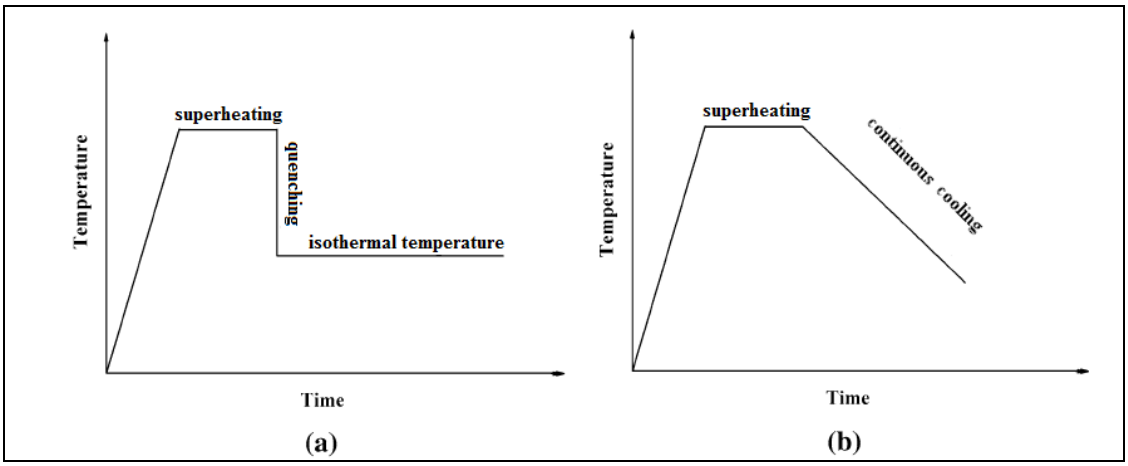

Figure 6. Typical thermal profiles to get data for TTT (a) and CCT (b) diagrams.

3. Results

3.1 CA slag

The *liquidus* temperature for this slag according to FactSage 6.1 is 1518 °C, and the first crystal during cooling is $CaAl_2O_4$. The second crystal during cooling is $Ca_3Al_2O_6$, which precipitates at 1362 °C, at *solidus* temperature.

For the lower cooling rates, in a few seconds after the start of crystallisation the sample seems to be completely crystalline, like at Figure 7c. A CCT diagram was built, Figure 8. The samples were maintained at 1700 °C during 1 minute before the cooling at different cooling rates. The triangles mean the point of first crystals precipitation. The crystallisation starts far from the *liquidus*. It can be seen that the crystallisation temperature is a function of the cooling rate. The critical cooling rate is 1700 °C/min, i.e. with higher cooling rates no crystal is observed.

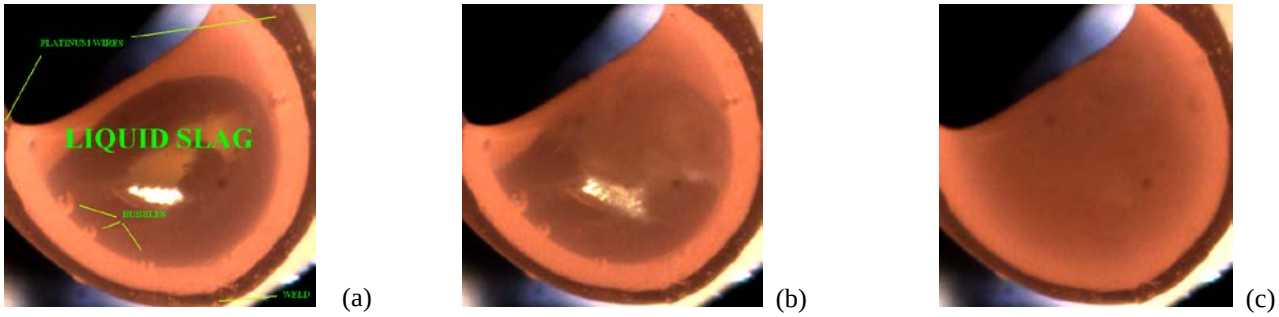

Figure 7. Slag CA at 30 °C/min from 1700 °C. (a) 1330 °C, no crystal; (b) 1292 °C, high %crystallinity; (c) 1280 °C, "full" crystallisation.

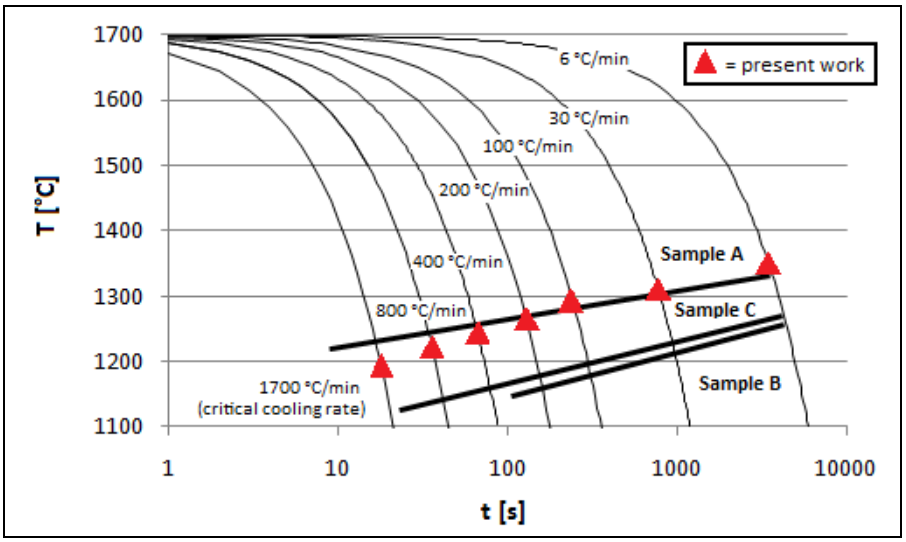

Figure 8. CCT diagram for the slag CA (43.7 %CaO, 56.3 %Al_2O_3), obtained from SHTT. The triangles mean the point of first crystals precipitation (crystallisation temperature) for the slag of the present work (44% CaO, 56% Al_2O_3). Samples A, B and C are calcium aluminate slags containing 48% CaO, 50% CaO and 53% CaO respectively, whose CCT diagrams were also determined through the hot thermocouple technique in a previous work [13].

3.2 CS slag

The slag $CaO.SiO_2$ with basicity (%CaO/%SiO_2) 0.7 , named here as CS, was studied. It has the following characteristics (FactSage 6.1): *liquidus* temperature 1500 °C, first phase during cooling $CaSiO_3$, *solidus* temperature 1437 °C, where the second crystal (SiO_2) precipitates.

Regarding CCT experiments, crystallisation is not observed even to very low cooling rates. The samples were completely melted, afterwards maintained at 1700 °C during 5 min, and then the cooling rates 30 °C/min and 10 °C/min were applied down to 700 °C.

Regarding TTT experiments, i.e. isothermal transformation, the samples were completely melted and afterwards maintained at 1700 °C during 5 min. Then a very high cooling rate (> 3000 °C/min) was applied. When the desired temperatures were reached – 900 °C, 950 °C, 1000 °C, 1050 °C, 1100°C, 1150°C, 1200 °C – the samples were maintained at the particular temperature up to 1000 s. Crystallisation was observed only at 1000 °C occurring at 76s (average for 6 experiments, standard deviation 27s) and was completed in few seconds.

Besides CCT and TTT experiments another kind of thermal cycle was applied: melting at 1700 °C, very high cooling rate (> 3000 °C/min) down to particular temperatures, maintenance during 60 s, and then heating again at 1000 °C/min up to 1700 °C. The particular temperatures studied in the present work were 900 °C, 950 °C, 975 °C, 1000 °C, 1025 °C, 1050 °C, 1100°C, 1150 °C, 1200 °C, and 1300 °C. It was observed considering this special thermal cycle that crystallisation occurs intensely during heating at 1000 °C/min, but only when starting (after quenching) at 1000 °C or below. The crystallisation occurs intensely in the range 1069 - 1125 °C when starting at 900 °C, 950 °C, 975 °C, and 1000 °C. Thus, it is clear that when increasing the temperature after reaching a particular range of lower temperatures good conditions for crystal growth can be obtained. At Figure 9 there is an example, which is the result of maintaining one sample at 900 °C during 60 s and then heating at 1000 °C/min.

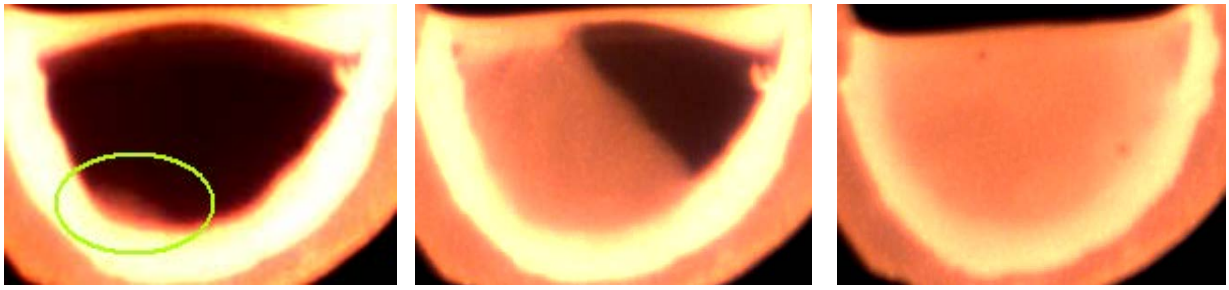

(a) (b) (c)

Figure 9. Crystallisation for a CaO-SiO_2 slag (B = 0.72) when increasing the temperature at 1000 °C/min, after maintaining the sample at 900 °C during 60 s; images got from SHTT. (a) 1079 °C, start of crystallisation (green circle); (b) 1202 °C, 7 s after the start of crystallisation; (c) 1297 °C, 13 s after the start of crystallisation (full crystallisation).

3.3 CST_1 slag

The slag of the system CaO-SiO_2-TiO_2 named here as CST_1 (41.1 %CaO, 29.1 %SiO_2, 29.8 %TiO_2) was used to study the effect of duration of superheating on incubation time. The *liquidus* temperature of this slag is very high, ca. 1600 °C. The first phase during cooling from liquid slag is CaO.TiO_2 . According to the composition triangle the possible phases are CaO.TiO_2, CaO.SiO_2, and CaO.SiO_2.TiO_2 [14].

For this study a special thermal cycle was used. Before the melting the samples were maintained at 1200°C during 60 s. Doing in this way the samples always seemed to be completely crystalline according to the SHTT observation. Then the following sequence was performed: (i) the samples were held in the range 1650 °C - 1680 °C during different holding times; (ii) quenching down to 1400 °C; (iii) measurement of the incubation times (when the first crystals can be observed). The samples always were visually completely melted and transparent for both holding times (60 s and 600 s).

It was observed that the duration of superheating changed completely the crystallisation behaviour of the slag CST_1, assuming that the initial conditions before melting were the same. When the holding time is 60 s the incubation times tend to be much shorter (5-12 seconds) than when the holding time is 600 s (no crystal observed up to 1000 seconds!). Two samples were analysed, one with 1.4 mg and the other with 2.3 mg.

At Figure 10 the isothermal tranformation at 1400 °C for the sample with 2.3 mg when the duration of the

superheating is 60 s.

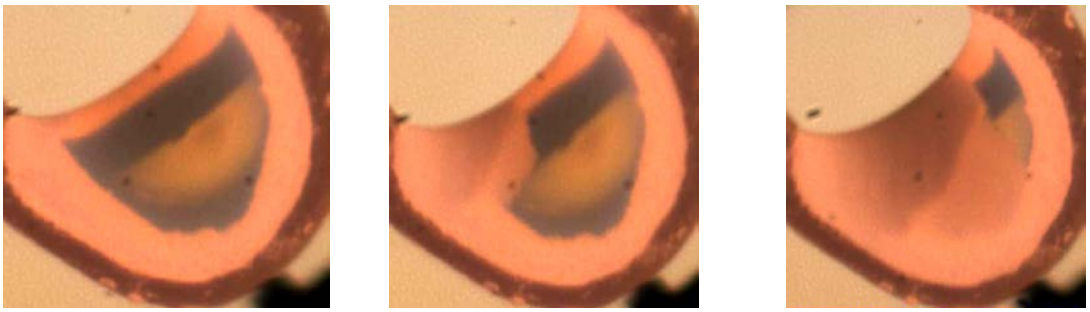

(a) (b) (c)

Figure 10. Crystallisation for the CST_1 slag (41.1 %CaO, 29.1 %SiO_2, 29.8 %TiO_2) at 1400 °C when the duration of the superheating is 60 s at 1650 °C - 1680 °C. After the quenching the measured incubation time is ca. 10 s. (a) no crystal, (b) and (c) crystallisation in progress.

3.4 CSTNA slags

TTT diagrams were built for the CSTNA slags. The slag samples were maintained at 1600 °C during 30 s after heating at 1000 °C/min. At this high temperature the samples are completely melted in a few seconds. It was clearly observed that if the same sample is used to do many determinations at the same temperature the incubation times became longer. The reason for this effect is Na_2O loss at high temperatures, assuming that the higher the %Na_2O content the higher the crystallisation tendency. To avoid this problem the maximum number of measurements per sample was ten. It can be seen at Figure 11 that Na_2O addition shortens intensely the incubation times from the CaO-SiO_2-TiO_2 slag system (comparing with composition at Table 1).

At Figure 11 it can be seen the TTT diagram of a commercial mould powder normally employed in the continuous casting of stainless steels, whose TTT diagram was also built using SHTT [15]. This commercial mould powder contains CaF_2 and Na_2O and does not contain TiO_2 .

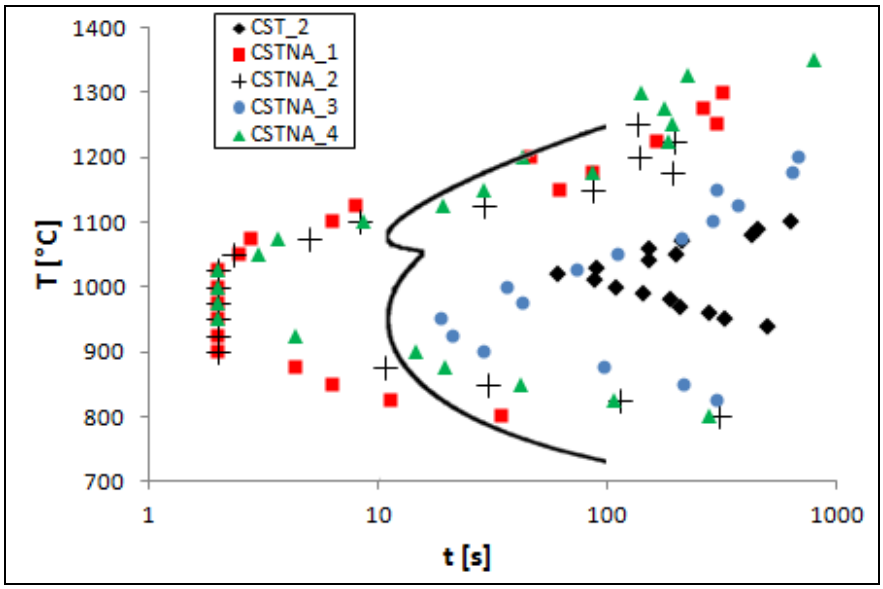

Figure 11. TTT diagrams for slags in the CaO-SiO_2-TiO_2-Na_2O-Al_2O_3 system (composition at Table 1) obtained from SHTT and for a F-bearing industrial slag from [15] (continuous line obtained also from SHTT).

Regarding crystals morphology, it was observed for all the slags that the morphology of the crystals varies with temperature. Two kinds of crystals were observed: columnar grains (which seem to grow unidirectionally from surface to centre of the sample) and equiaxed grains (which seem to grow radially in the liquid slag). It was reported that, for crystallisation in mould fluxes, both columnar and equiaxed grains grow dendritically [16].

Crystals show dendritic structure at higher temperatures and become small and dense at lower temperatures. For these last ones, which are formed in the middle of the liquid slag for higher degree of undercooling, they can be explained by homogeneous nucleation.

At Figure 12a it is shown an image of one slag completely liquid at 1600 °C, with the lamp below the sample off. For all the experiments the lamp below the sample was turned on, because in this way the resolution image is higher. At higher temperatures (Figures 12b and 12c) it is common to observe dendrites nucleating from thermocouple borders or sample borders. These temperatures correspond to long incubation times and consequently to lower crystallisation rates. At lower temperatures (Figures 12d and 12e) there are equiaxed grains growing from different points in the sample. At 900 °C the samples are translucent, Figure 12f. The incubation time is 2 seconds and the samples are completely opaque in only 4 seconds. The crystals are very fine and the density of crystals increased until it appeared “cloud-like” (a similar result is reported in [17] p. 433).

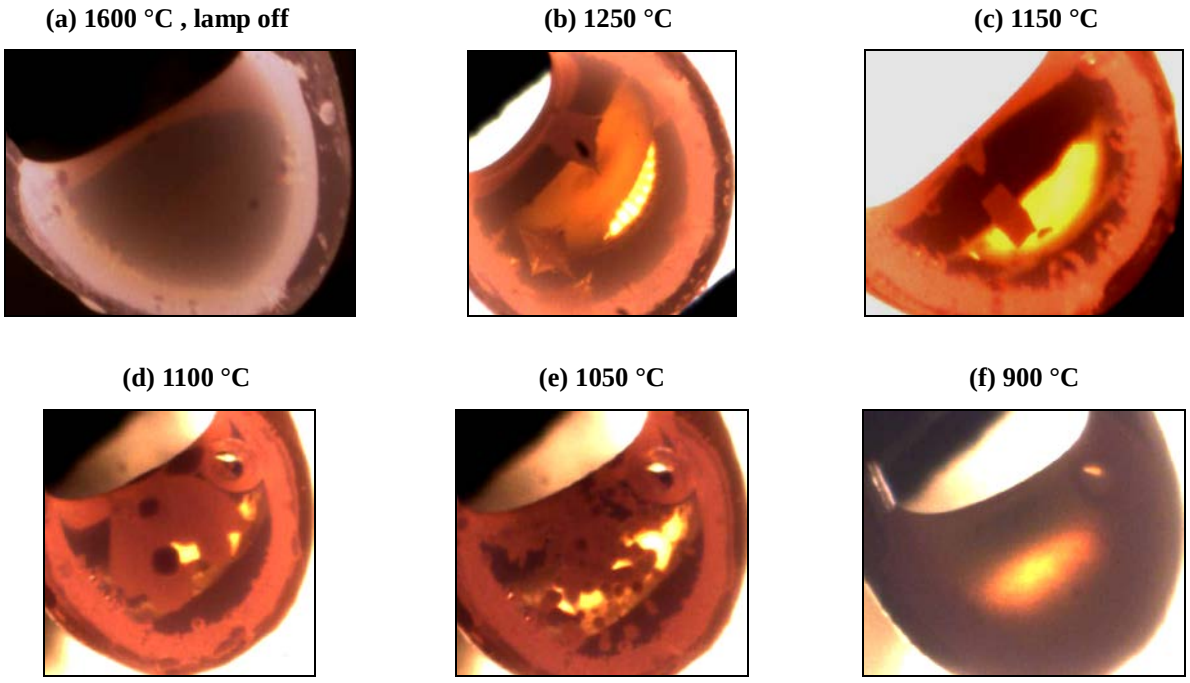

Figure 12. Images from experiments performed with the slag CSTNA_1 at different temperatures.

4. Discussion

4.1 CA slag

Prapakorn and Cramb [13] showed CCT diagrams for calcium aluminate slags which were named as Sample A = 48% CaO, Sample B = 50% CaO and Sample C = 53% CaO, see Figure 8. The CCT diagrams for these slags were also

determined through the hot thermocouple technique. According to their observations it is easiest to form a glass at the eutectic composition, i.e. 50% CaO. The slag CA studied in the present work has got 44% CaO and presents a CCT curve more similar to Sample A. Thus, the comparison with these results is coherent.

4.2 CS slag

For the $CaO\text{-}SiO_2$ slag (B=0.7) no crystal was detected during experiments with SHTT at continuous cooling rate, even to very low cooling rates. This result agrees with other reported results for $CaO\text{-}SiO_2$ slags with basicity 0.8, 1.0 and 1.2, where also no crystal was detected when doing CCT experiments [11].

However, it was observed that it is possible to get intense crystallisation for a low basicity $CaO\text{-}SiO_2$ slag, depending on the thermal cycle. The explanation for this intense crystallisation can be the fact that the optimum range of temperatures for crystal nucleation is lower than the optimum range of temperatures for crystal growth. Because of that crystals cannot be detected through CCT experiments even to very low cooling rates. This idea makes sense considering that the rate of crystal growth is not the only factor determining the abilitity of a melt to form crystals, since crystals grow from a certain number of nuclei, and in many respects the nucleation stage determines the pathways of overall crystallisation in silicate glasses [18].

It is well-known that crystallisation can be divided in two processes: (i) formation of nuclei and (ii) crystal growth. The rates of both processes are temperature-dependent with maxima at certain supercooling values. These maxima are separated in glass-forming materials suitable for preparation of glass ceramics permitting control of the glass crystallisation [19].

The observation of crystals during isothermal experiments at 1000 °C for the slag CS is explained by the fact that this is an intermediate temperature, where both nucleation rate and growth rate are sufficiently high.

4.3 CST_1 slag

It is known that the new phase is nucleated by nuclei which already exist in the old phase and whose effective number per unit nucleation region can be altered by temperature and duration of superheating. There are indications that, for given supercooling or superheating, the nuclei grow or diminish considerably more slowly than grains of visible size. These nuclei, which may be heterogeneities of any sort, would usually consist of small particles of the subcritical phase or tough films of the latter surrounding foreign inclusions [20].

Thus, it can be concluded that there is a relation between the duration of superheating, incubation times, and number of nuclei. The longer the superheating, the lower the number of nuclei per unit nucleation region and consequently the longer the incubation time.

According to Avrami experimental observations [20], at any temperature the nuclei grow (supercooling) or diminish (superheating) more slowly than grains of measurable size (in the μm range). This tendency was confirmed for nuclei growth, i.e. supercooling [21]. The crystallisation behaviour of the $Li_2O.2SiO_2$ glass was studied with special emphasis in the induction period for crystallisation. It was demonstrated for this glass, which crystallise through homogeneous

nucleation, that the times required to grow super-critical nuclei (nm range) to sizes detectable by optical microscopes (μm range) are long, appearing as induction times in lenght versus time plots. The apparent induction periods determined by three independent kinetic measurements were in the range 1-4 hours. The glassy samples were maintained at 500 °C during 75 h, reaching up to 26% volume crystal fraction. It was concluded that the time required for the first crystal to grow to detectable sizes is the main component of the experimental apparent observed induction periods.

4.4 CSTNA slags

Na_2O has an important role, related to crystallisation tendency. The TTT diagrams show that it is possible to control the crystallisation tendency changing the Na_2O content.

The effect of Na_2O content on incubation times was reported using the Hot Thermocouple Technique for simple slags with $\%CaO/\%SiO_2$ =1 and $\%Al_2O_3$ in the range 6%-7%. It was shown that Na_2O in the range 2-7% shortens the incubation times [22, 23].

Na_2O also has an important role regarding mould slag viscosity. It is known that the lower the viscosity the easier the crystallisation. At Figure 13 a summary for viscosity measurements for the CS, CST_2 and CSTNA_1 slags which were performed in the Institute of Iron and Steel Technology of the Freiberg University of Mining and University [24].

It can be seen for the range of temperatures that:

(i) when adding TiO_2 into a CS slag with binary basicity = 0.8 , the viscosity decreases, and

(ii) afterwards, when adding Na_2O into the CST_2 slag the viscosity decreases more.

Samples were collected after the viscosity measurements and analysed by X-ray fluorescence. At Table 3 the variation in the composition , comparing before and after the experiments.

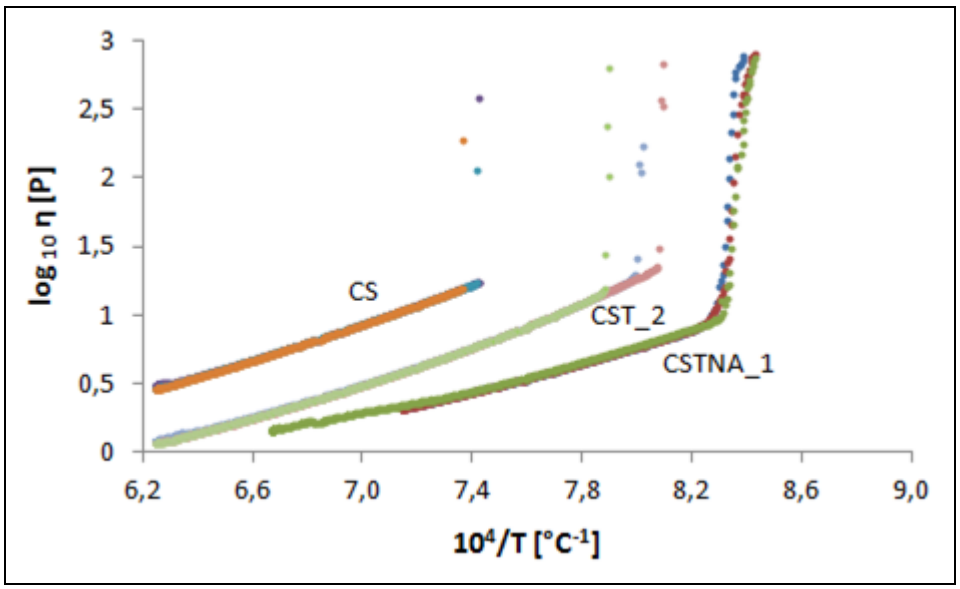

Figure 13. Viscosity measurements with rotation viscometer (three samples per composition).

Table 3. Variation in the composition for viscosity measurements, comparing before and after the experiments [%wt].

	%CaO	%SiO_2	%TiO_2	%Na_2O	%Al_2O_3
CA	0.2				-0.2
CS	0.2	-0.2			
CST_2	0.2	-0.2	0.0		
CSTNA_1	0.0	0.4	0.0	-0.4	

For the slag CS the sudden increase of the viscosity at Figure 13 is surprising, because during the experiments with CCT no crystal was observed at 10 °C/min using the SHTT, i.e. with the same continuous cooling rate used for the viscosity measurements. This increase of the viscosity should be related to precipitation of crystals. For this CS composition above 870 °C it is possible to have wollastonite, $CaO.SiO_2$, and tridymite, SiO_2 [14]. The precipitation of small transparent crystals at high temperature, not visible for the present experimental conditions, would explain this situation.

Since the Ti^{4+} cation is larger than the Si^{4+} cation, the Ti-O-Al and Ti-O-Ti bonds are expected to be weaker than Si-O-Al and Si-O-Si bonds. Therefore, the addition of TiO_2 to highly polymerized aluminosilicate melts will decrease their viscosity, although the overall NBO/T ratio decreases with increasing TiO_2 content of the melt. This deduction from structural considerations is consistent with rheological data for TiO_2-bearing aluminosilicate melts [25].

For sodium silicate glasses, the atom ratio O/Si is greater than 2. Therefore, part of the oxygen atoms are bonded between two silicon atoms and part to only one silicon atom. There is a gradual breakdown of the silicate network with the addition of Na_2O to molten silica [25, 26].

Industrial mould slags would be more complex than the CSTNA slags, since they have more components. Anyway, the present study can be used as a reference for future developments when designing fluorine-free mould powders for slab casting, where the control of crystallisation is imperative.

5. Conclusions

(i) for the slag CS (B=0.7) the crystallisation is much more intense when increasing the temperature after reaching lower temperatures (< 1000 °C), according to SHTT observations. The optimum range of temperatures for crystal nucleation is lower than the optimum range of temperatures for crystal growth.

(ii) for the CST_1 slag, which has high *liquidus* temperature (ca. 1600 °C) it was found that the longer the superheating (in the range 1650 °C - 1680 °C) the longer the incubation times, i.e. the duration of the superheating for a slag – which seems to be completely liquid – can affect strongly the crystallisation behaviour for this slag. The explanation for the crystal growth would be the fact that invisible nuclei (in the nm range) diminish more slowly than grains of measurable size (in the μm range).

(iii) it was found that the addition of Na_2O into the CaO-SiO_2-TiO_2 slag system shortens intensely the crystals incubation times at TTT diagrams to the range of seconds. Therefore Na_2O increases the crystallisation kinetics. It is possible to control the crystallisation behaviour changing the Na_2O content.

Acknowledgements

The author Jeferson L. Klug wishes to express his gratitude to the Brazilian Science and Technology National Council (CNPq) for the granted scholarships, and gratefully acknowledge the support from the company Stollberg do Brasil.

References

[1] Mills, K., *The making, shaping and treating of steel (chapter 8)*. 2003, The AISE Steel Foundation: Pittsburgh.

[2] Kromhout, J.A., *Mould powders for high speed continuous casting of steel*. 2011, PhD dissertation, Technische Universiteit Delft.

[3] Hooli, P., *Study on the layers in the film originating from the casting powder between steel shell and mould and associated phenomena in continuous casting of stainless steel*. 2007, PhD dissertation, Helsinki University of Technology.

[4] Nakada, H. and K. Nagata, *Crystallization of $CaO–SiO_2–TiO_2$ slag as a candidate for fluorine free mold flux.* ISIJ International, 2006. **46**(3): p. 441-449.

[5] Wen, G., Sridhar, S., Tang, P., Qi, X., Liu, Y., *Development of fluoride-free mold powders for peritectic steel slab casting.* ISIJ International, 2007. **47**(8): p. 1117-1125.

[6] Qi, X., G. Wen, and P. Tang, *Investigation on heat transfer performance of fluoride-free and titanium-bearing mold fluxes.* Journal of Non-Crystalline Solids, 2008. **354**: p. 5444-5452.

[7] He, S., Wang, Q., Xie, D., Xu, C., Li, Z., Mills, K. C., *Solidification and crystallization properties of $CaO-SiO_2-Na_2O$ based mould fluxes.* International Journal of Minerals, Metallurgy and Materials, 2009. **16**(3).

[8] Wang, Q., S. He, and K.C. Mills, *Research on decreasing fluorine content from continuous casting mould fluxes*, in *4^{th} International Conference on Continuous Casting of Steel in Developing Countries*. 2011: China.

[9] Zhang, Z., G. Wen, and Y. Zhang, *Crystallization behavior of F-free mold fluxes.* International Journal of Minerals, Metallurgy and Materials, 2011. **18**(2, April 2011).

[10] Choi, S., Lee, D., Shin, D., Choi, S., *Properties of F-free glass system as a mold flux: viscosity, thermal conductivity and crystallization behavior.* Journal of Non-Crystalline Solids, 2004. **345&346**: p. 157-160.

[11] Lachmann, S. and P.R. Scheller, *Effect of Al_2O_3 and CaF_2 on the solidification of mould slags and the heat transfer through slag films*, in *VIII International Conference on Molten Slags, Fluxes and Salts*. 2009: Santiago, pp. 1101.

[12] Patnaik, P., *Handbook of inorganic chemicals*, McGraw-Hill, Editor. 2003.

[13] Prapakorn, K. and A.W. Cramb, *Initial solidification behavior in continuous casting: the effect of MgO on the solidification behavior of $CaO-Al_2O_3$ based slags*, in *MS&T Conference Proceedings*. 2004.

[14] VDEh, ed. *Slag Atlas - 2nd edition*. 1995.

[15] Kashiwaya, Y., C.E. Cicutti, and A.W. Cramb, *An investigation of the crystallization of a continuous casting mold slag using the Single Hot Thermocouple Technique.* ISIJ International, 1998. **38**(4): p. 357-365.

[16] Mizuno, H., Esaka, H., Shinozuka, K., Tamura, M., *Analysis of the crystallization of mold flux for continuous casting of steel.* ISIJ International, 2008. **48**(3): p. 277-285.

[17] Seetharaman, S., ed. *Fundamentals of metallurgy*. 2005, Woodhead Publishing and Maney Publishing on behalf of The Institute of Materials, Minerals and Mining.

[18] Fokin, V.M., Zanotto, E. D., Yuritsyn, N. S., Schmelzer, J. W. P., *Review - homogeneous crystal nucleation in silicate glasses: a 40 years perspective.* Journal of Non-Crystalline Solids, 2006. **352**: p. 2681-2714.

[19] Strnad, Z., *Glass-ceramic materials*. Glass Science and Technology. Vol. 8. 1986: Elsevier Science Publishing

Company.

[20] Avrami, M., *Kinetics of phase change (Part II) - transformation-time relations for random distribution of nuclei.* Journal of Chemical Physics, 1940. **8**(February): p. 212-224.

[21] Zanotto, E.D. and M.L.G. Leite, *The nucleation mechanism of lithium dissilicate glass revisited.* Journal of Non-Crystalline Solids, 1996. **202**: p. 145-152.

[22] Mutale, C.T., T. Claudon, and A.W. Cramb, *Observation of the crystallization behavior of a slag containing 46 wt pct CaO, 46 wt pct SiO_2, 6 wt pct Al_2O_3, and 2 wt pct Na_2O using the Double Hot Thermocouple Technique.* Metallurgical and Materials Transactions B, 2005. **36B**(June 2005).

[23] Kashiwaya, Y., Cicutti, C. E., Cramb, A. W., Ishii, K., *Development of Double and Single Hot Thermocouple Technique for in situ observation and measurement of mold slag crystallization.* ISIJ International, 1998. **38**(4).

[24] Wu, L., *Viscosity measurements of slags with rotation viscometer*, in *Institute of Iron and Steel Technology*. 2011, Diplomarbeit, Freiberg University of Mining and Technology: Freiberg.

[25] Turkdogan, E.T., ed. *Physicochemical properties of molten slags and glasses*. 1983, The Metals Society, London.

[26] Callister, W.D., *Materials science and engineering - an introduction (second edition)*.